Journal of Achievements in Materials and Manufacturing Engineering
VOLUME 29
ISSUE 1
July
2008

Austenite formation during intercritical annealing

J. Lis, A. Lis *
Institute of Materials Engineering, Czestochowa University of Technology,
Al. Armii Krajowej 19, 42-200 Częstochowa, Poland
* Corresponding author: E-mail address: lis@mim.pcz.czest.pl

Received 30.03.2008; published in revised form 01.07.2008

Manufacturing and processing

ABSTRACT

Purpose: of this paper is the effect of the soft annealing of initial microstructure of the 6Mn16 steel on the kinetics of the austenite formation during next intercritical annealing.
Design/methodology/approach: Analytical TEM point analysis with EDAX system attached to Philips CM20 was used to evaluate the concentration of Mn, Ni and Cr in the microstructure constituents of the multiphase steel and mainly Bainite- Martensite islands.
Findings: The increase in soft annealing time from 1-60 hours at 625°C increases Mn partitioning between ferrite and cementite and new formed austenite and decreases the rate of the austenite formation during next intercritical annealing in the ($\alpha+\gamma$) temperature range at 700 and 750°C. The general equations for carbide dissolution and austenite formation in intercritical temperature range were established.
Research limitations/implications: The final multiphase microstructure can be optimised by changing the time / temperature parameters of the intercritical heating in the ($\alpha+\gamma$) temperature range.
Originality/value: The knowledge of partitioning of alloying elements mainly Mn during soft annealing and intercritical heating is very important to optimise the processing technology of intercritical annealing for a given amount of the austenite.
Keywords: Heat treatment; Soft and intercritical annealing; Mn partitioning; Austenite formation

1. Introduction

Problem of the austenite formation during intercritical annealing of low carbon medium manganese steel has been less studied than mechanisms and kinetics of the austenite phase transformations on cooling from full austenitization temperature or the ($\alpha+\gamma$) temperature range and after controlled deformations [1-9]. In the current research of the intercritical heating of 6Mn16 steel in the ($\alpha+\gamma$) temperature range, it has been assumed that Mn diffusion in ferrite is much faster than in austenite. However for equilibrium partitioning of Mn between ferrite and austenite in low carbon manganese steel very long time of heating is needed. It was mentioned in paper [10] that for steel having 0.11 wt.% C and 2.67 wt.% Mn which was annealed in the ($\alpha+\gamma$) temperature range at temperature 680°C after 10^8 s the equilibrium balance was achieved for Mn partitioning between ferrite and austenite. Thus to decrease that time markedly soft annealing below A_{C1} temperature at 625°C for 1-60 hours was applied to the investigated steel after controlled rolling [11, 12, 19]. Purpose of that treatment was to activate Mn diffusion in the ferrite matrix and Mn enrichment process in the cementite and bainitic carbides.

2. Material and investigation methods

The chemical composition of the investigated 6Mn16 steel was 0.047 wt.% C, 3.97 wt.% Mn, 0.37 wt.% Si, 0.003 wt.% P, 0.009 wt.% S, 0.01 wt% Cr, 0.17 wt.% Ni, 0.02 wt.% Mo, 0.02

wt.% Cu, 0.02 wt.% Nb, 0.017 wt.% Ti. The steel, after heating at 1172°C for two hours was controlled rolled into plates of 12 mm in thickness. The critical temperatures of diffusional phase transformations on heating were A_{C1}= 647°C and A_{C3}= 850°C.

The dilatometric investigations were performed with dilatometer Bähr DIL 805 and DO 105 with transducer for expansion/contraction measurements of the sample length. Electronic signal was calibrated with computer, so amount of newly formed austenite was measured during continuous intercritical annealing at 700°C and 750°C for 1800 s. Also some amount of austenite was detected during soft annealing at temperature 625°C for duration 10 and 60 hours.

3. Description of achieved results and discussion

The results of the effect of the soft annealing time at 625°C on microsegregation of Mn and Si between ferrite matrix and carbides and locally austenite islands are presented in Table 1.

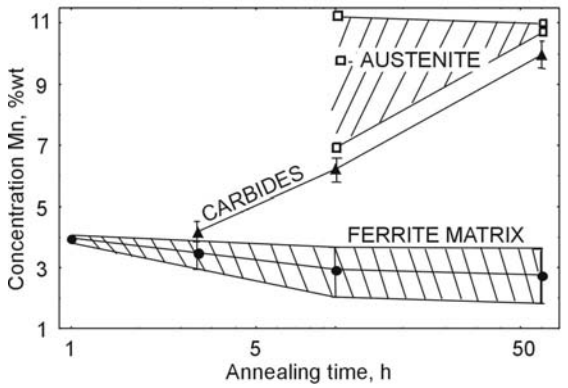

Fig. 1. Manganese concentration changes in structural constituents of 6Mn16 steel with annealing at 625°C

The partitioning effect of Mn between carbides and retained austenite increased with the increase in duration time of soft annealing from 3 to 60 hours, what is presented in Fig. 1.

In ferrite matrix continuous decrease in Mn concentration was observed with increase in time of soft annealing process while in carbides and residual austenite the concentration was increased.

The effect of Mn partitioning between ferrite and austenite was calculated for 6Mn16 steel with Thermo-Calc program for different temperatures of heat treatment in the ($\alpha+\gamma$) range. The results are presented in Table 2. They are compared to experimental data of Mn segregations between ferrite and austenite determined by microsegregation studies on thin foils with analytical STEM point analysis in Fig. 2.

By simulation of soft annealing of 6Mn16 steel at 625°C with program Thermo-Calc for conditions of thermodynamic equilibrium it was possible to foresee that microstructure will consist of 86.3% of ferrite with 2.86 wt.% Mn and 13.4 % of austenite with 11.2 wt.% Mn and small amounts of MC and M_3C carbides i.e. $(FeMn)_3C$ with 1.60 wt.% Mn. This result allows to foresee the direction of the changes in microstructure for given temperature, time and alloying concentrations in the steel. Thus the detected highly alloyed with Mn carbides will dissolve in the surrounding austenite increasing its concentration to 11.2 wt.% Mn while alloyed cementite will stay at 1.6 wt.% Mn. That dissolution process of alloyed carbides in newly formed austenite probably had an effect on discrepancies between calculated and measured experimental values of Mn concentrations shown in Fig. 2. The increased concentrations of Mn at 625°C for 10 and 60 hours will affect local decrease of A_{C1} temperature thus austenite islands may rise. The formation of residual austenite was confirmed with X-ray analysis and by observations of bainite- martensite islands on thin foils of rapidly cooled samples from 625°C as an effect of phase transformations of the new austenite to martensite. It was confirmed that soft annealing at 625°C activates Mn diffusion in the ferrite matrix and Mn enrichment process in cementite. On the other hand saturation of carbides with Mn will change their dissolution process during next intercritical annealing heating and may also change kinetics of austenite formation in the ($\alpha+\gamma$) range.

Table 1.
Effect of annealing time at 625°C on alloying elements concentration in structural components of the 6Mn16 steel

Alloying element	Annealing time, hours							
	3	10	60	3	10	60	10	60
	Concentration of element in % wt.							
	Ferrite matrix			Carbides			Austenite	
Si	0.44	0.4-0.57	0.36-0.61	0.36	0.15-0.33	0.15-0.31	-	-
Mn	3.5	2.06-3.81	1.9-3.5	4.0-4.35	5.73-6.69	9.69-10.2	7.0 - 11.2	10.7 – 11.3
Average Mn	3.5	2.93	2.70	4.18	6.21	9.95	9.1	11.0

Table 2.
Thermo-Calc calculations of Mn partitioning between ferrite and austenite of 6Mn16 steel for given temperature

Temperature, °C	α - Fe, wt.% Mn	γ - Fe, wt.% Mn
625	2.86	11.20
700	2.413	6.925
750	1.967	4.617
780	1.80	4.0
Ac_3	-	3.97

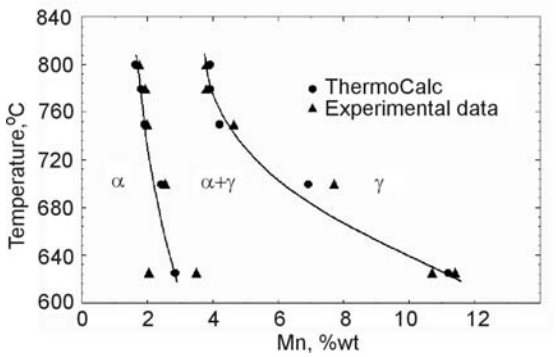

Fig. 2. Partition of Mn between ferrite and austenite of 6Mn16 steel

Final TRIP assisted multiphase microstructure of 6Mn15 steel can be optimised by changing time/ temperature parameters of the intercritical heating. Thus progress of austenite formation was studied to establish conditions of heat treatment for 20-35% of austenite in the structure.

This amount of austenite is needed for creation of the multiphase ferrite-martensite and retained austenite microstructure after fast cooling from (α+γ) temperature range. Temperatures 700 and 750°C and time 1800 s were selected for austenite progress studies.

In Fig. 3 the effect of soft annealing pre-treatment on the amount of austenite formed after 1800 s at 700°C is presented and compared to the kinetic of austenite formation during immediate annealing after controlled rolling of the steel. The fastest progress of austenite formation was observed at immediate annealing. The longer time of the soft annealing the slower is kinetics of the austenite creation during intercritical annealing at 700°C. During immediate annealing at 700°C 20% of austenite was achieved after 90 s while 25% after 112 s and 30% after 150 s. Phase transformation of bainitic microstructure into austenite is quite fast during continuous heating at rate 0.6°C/s up to temperature 700°C. 35% of new austenite was determined from dilatometric studies after 200 s.

However, soft annealing at 625°C intensified Mn partitioning. Saturation of carbides with Mn caused their slower dissolution and reduced the progress of α→γ transformation as well as grain growth. It was found that for 20% of new austenite formation which was rich in C and Mn the increase in time from 90 to 708 s was observed after soft annealing 3600 s at 625°C and intercritical treatment 700°C/1800 s.

These long times of intercritical annealing allows for easy control of the intercritical heat treatment at 700 ^{0}C. For the increased duration of the soft annealing at 625 ^{0}C to 36 ks the delay in α→γ transformation progress at the level of 20% of austenite was 1260 s and for 216 ks was 1780 s.

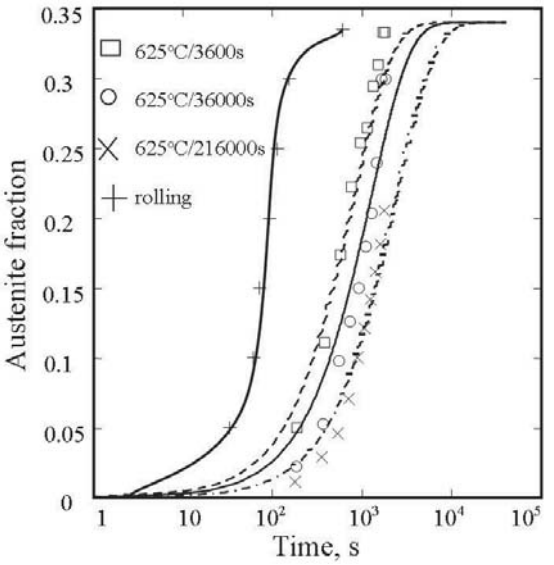

Fig. 3. Effect of annealing time at 625^{o}C on the increase austenite fraction in 6Mn16 steel after annealing at 700^{o}C for 1800 s compared to immediate annealing after rolling

These kinetics of α→γ phase transformation were described with Avrami, Johnson-Mehl equations [13-15]. From experimental data which are presented in Fig. 3 the value n=1 in J-M equations was established. Thus from mathematical simulations of the progress of phase transformation curves the constant parameter "k" values, which represented the rate of transformation were determined as: $k_{3600}=12*10^{-4}$ and $k_{36ks}= 8*10^{-4}$.

Progress of the diffusional phase transformation is determined by the movement of interphase boundaries; so k=1/t where

$$t=t_{Xv}=t_{0.215} \quad (1)$$

at condition n=1 in equation J-M and standardisation that 0.34 relates to 100% of the total progress of α→γ transformation at 700 ^{0}C one achieves

$$Y= 1- \exp-(kt)^n \text{ and } Y=X_v \quad (2)$$

$$X_v=1- \exp-(kt)^n=0.34 \quad (3)$$

t_{Xv} – time for fraction of transformation X_v
k – constant for transformation rate

In Fig. 4 there are presented the progresses of α→γ transformation at 750°C for immediate annealing the bainite microstructure of 6Mn16 steel after controlled rolling and after pre-treatment of soft annealing at 625°C for 3600 s and 36 ks. Time for formation of 20% and 50% of austenite was studied. For bainite microstructure time for reaching 20% of austenite and 80% of ferrite was 100 s, while after soft annealing 625°C for 3600 s was 280 s and that for 625°C/36 ks was 500 s.

The increased temperature 750°C makes easier Mn diffusion partitioning between ferrite and austenite. For formation of duplex structure 50% α +50%γ only 189 s is needed during immediate annealing after controlled rolling and after soft annealing 700 s or

1400 s – Fig. 4. Assuming that phase transformation mechanism of $\alpha \rightarrow \gamma$ at temperature 750°C is analoguos to that at 700°C and value n=1 the values of k in equations of J-M were calculated to be $k_{3600}=15*10^{-4}$ and $k_{36ks}=9*10^{-4}$.

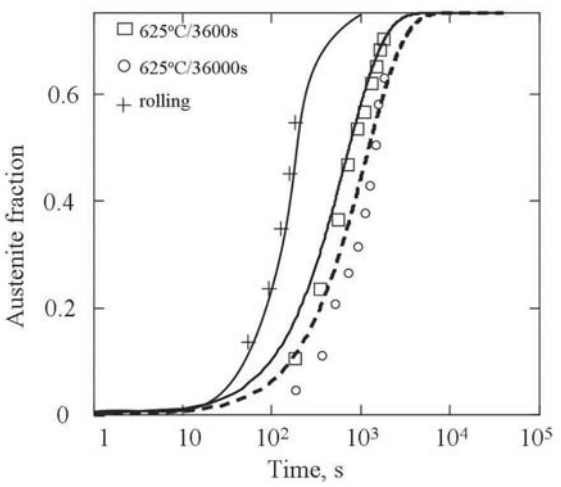

Fig. 4. Effect of annealing time at 625°C on the fraction of austenite in 6Mn16 steel after annealing at 750°C fir 1800s compared to immediate annealing after rolling.

For thermodynamic equilibrium at temperature 750°C, 75% of austenite may be formed with concentration of 4.62 wt.% Mn. This is slightly higher than average concentration of Mn in the steel. So that is the reason why small amount of retained austenite is observed in duplex microstructures after quenching the steel and why small TRIP effect is observable for the final product.

4. Model of diffusional carbide dissolution and austenite formation during intercritical treatment

It was assumed that carbides have spherical or pencil shape and they are dissolving in surrounding austenite matrix during isothermal heating in $\alpha+\gamma$ temperature range accordingly to situation presented in Fig. 5. The principles of the model were based on Goodman (HBIM) – heat balance integral method [17]. Spherical particles with average mean radius r_0 are homogenously distributed at distance 2L. The particle radius is changing with the time r=x(t) and after $t=t_C$ diffusion field $\delta(t)$ may reach an extension $L = x(t) + \delta(t)$.

Dissolution process for dissolution time $t < t_c$ is given by equation

$$\frac{\partial C}{\partial t} = D\left(\frac{\partial^2 C}{\partial r^2} + \frac{2}{r}\frac{\partial C}{\partial r}\right) \tag{4}$$

at diffusivity $D = D_T$ = const and boundary conditions:
$C_S = C(r, t)$ $r = x(t)$ $t \geq 0$

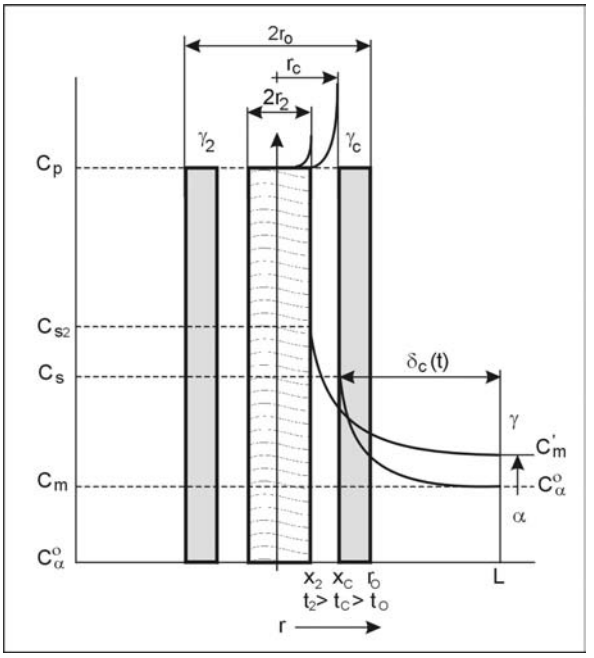

Fig. 5. Scheme of concentration profiles after different times $t_z > t_c > t_0$ of carbide dissolution in surrounding austenite
C_P – carbon concentration or Mn in $(FeMn)_3C$,
C_S – concentration of diffusing element from carbide surface into interface $0 < C_S < 1$,
C_m – element concentration in austenite matrix,
C_α^0 - element concentration in α phase,
r_o – starting radius of particle,
r_z – radius after time t_z; $r = t(x)$,
$\delta_c(t)$ – depth of penetration of diffusion field from dissolving particle

$C_P = C(r, t)$ $r_o \leq r < x(t)$

$$\frac{\partial C}{\partial r} = 0 \qquad r = L$$

$$D\left.\frac{\partial C}{\partial r}\right|_{r=x(t)} = (C_P - C_S)\frac{dx}{dt} \tag{5}$$

where: x(t) determines the moving front of the interface carbide/ austenite.

After standardisation: concentration $C_P = 1$ and $C_m = 0$ concentration in matrix not being influenced by diffusional fields. So C_S is changing from 0 to 1. Conditions for moving boundary after differentiating of C_S versus time and applying (4) and (5) are given by relation (6) for time $t < t_c$ and $r = x(t)$

$$-(C_P - C_S)\left(\frac{\partial^2 C}{\partial r^2} + \frac{2}{r}\frac{\partial C}{\partial r}\right) = \left(\frac{\partial C}{\partial r}\right)^2 \tag{6}$$

Kinetics of diffusional front which moves in the range $x(t) < r \le L$ is described by equation (7)

$$\int_{x(t)}^{L} \frac{\partial C}{\partial t}\,dr = D \int_{x(t)}^{L} \left(\frac{\partial^2 C}{\partial r^2} + \frac{2}{r}\frac{\partial C}{\partial r} \right) dr \qquad (7)$$

or in the form of the relation (8)

$$\frac{d}{dt}\left\{ \int_{x(t)}^{L} C(r,t)dr - 2D \int_{x(t)}^{L} \frac{dC}{r} + C_S \frac{dx}{dt} + D\frac{\partial C}{\partial r}\Big|_{r=L} \right\} = 0 \qquad (8)$$

Profile of the distribution of chemical concentrations was assumed to be polynomial function of third power as in (9)

$$C(r,t) = C_S - A_1 \frac{r-x}{L-x} - \frac{A_2}{2}\left(\frac{r-x}{L-x}\right)^2 - \frac{A_3}{3}\left(\frac{r-x}{L-x}\right)^3 \qquad (9)$$

For $x(t) < r \le L$ there is analytical resolution. Parameters A_1, A_2, A_3 are determined from (5) and (6) applied into equation (9). The following boundary conditions were set for the depth of diffusion field $\delta(t)$, which are presenting profile of concentration in the matrix C_m beginning from dissolving particle to the value L for time $t = t_c$

$$x(t) + \delta(t) = L \qquad \text{dla } t = t_c \qquad (10)$$

$$\frac{\partial C}{\partial r} = 0 \qquad \text{dla } x(t) + \delta(t) \qquad (11)$$

$$C(r,t) = Cm \text{ dla } r = x(t) + \delta(t) \qquad (12)$$

Equation of the diffusion field is changed to one dimensional form by introduction a new parameter „ a = Cr ”

$$\frac{\partial a}{\partial t} = D\frac{\partial^2 a}{\partial r^2} \qquad (13)$$

and for conditions $a(x, t) = C_S$ for $t \ge 0$

$$D\left(x\frac{\partial a}{\partial r} - a \right) = x^2 \frac{dx}{dt}\left(C_P - C_S\right) \text{ for} = x(t) \qquad (14)$$

$$-\left(C_P - C_S\right) x \frac{\partial^2 a}{\partial r^2} = \left(\frac{\partial a}{\partial r} - \frac{a}{x} \right)^2 \quad r = x(t) \qquad (15)$$

The condition for moving masses for time $t < t_c$, it means for not overlapping diffusional fields after integration of eqauation (15) gives relationship (16)

$$\int_{x(t)}^{x(t)+\delta(t)} \frac{\partial a}{\partial t}\,dr = D \int_{x(t)}^{x(t)+\delta(t)} \frac{\partial^2 a}{\partial r^2}\,dr \qquad (16)$$

$$\frac{d}{dL}\left\{ \int_{x(t)}^{x(t)+\delta(t)} a(r,t)dr + x\,C_S \frac{dx}{dt} + D\frac{\partial a}{\partial r}\Big|_{r=x(t)} \right\} = 0$$

For numerical resolution of the above equation variable „a” was presented as polynomial of the third order

$$a \equiv \frac{2\,x\,C_S}{\delta^2}\left[r - (x+\delta)\right]^2 + \frac{3\,x\,C_S}{\delta^3}\left[r - (x+\delta)\right]^3 \qquad (17)$$

For $t = 0$, $x(t) = r_o$ and non-dimensional time constant τ the resolution is given as equations (18) and (19). They describe kinetics of dissolution of spherical particle in infinite matrix

$$x(t) = r_o - \left(\frac{D\,t}{\tau} \right)^{1/2} \qquad (18)$$

$$\tau = \frac{\alpha \cdot A^2 \cdot A_1^2}{8(1 + A_1)^2} \qquad (19)$$

Parameter α takes into account effect of Gibbs – Thompson [18] for small particles (20)

$$\alpha = 2{,}4 + \frac{2}{A}\left(2{,}4 + \frac{1}{A_1} \right)\left(1 + \frac{1}{A_1} \right) \qquad (20)$$

Constant A and A_1 for over saturation state are given by:

$$A = \frac{2\left(1 - C_S\right)}{C_S} \qquad (21)$$

$$A_1 = -\frac{1 + A^{1/2}}{1 - A} \qquad (22)$$

The critical time for overlapping of diffusional layers may be counted from equations (23) and (24):

$$t_c = \frac{\left(L - r_o\right)^2}{D\left[(2\alpha)^{1/2} - \frac{1}{\sqrt{\tau}} \right]^2} = \frac{\left(L - r_o\right)^2}{D\left[\sqrt{2}\,\alpha^{1/2} - \tau^{1/2} \right]^2} \qquad (23)$$

$$\left(\frac{D \cdot t_c}{r_o^2} \right) \equiv \frac{\left(1/f_o^{\,1/3} - 1 \right)^2}{\left[(2\,\alpha)^{1/2} - \tau^{1/2} \right]^2} \qquad (24)$$

where f_o is primary volume fraction of particles (25)

$$f_o = \left(\frac{r_o}{L}\right)^3 \tag{25}$$

On the other hand assuming that interface surface is stationary, ie. diffusion field has no memory of the previous position of the interface; Whelan [18] gave resolution for the rate of dissolution of the spherical particle at constant temperature (26):

$$\frac{dr}{dt} = \alpha\left[\frac{D}{r} - \sqrt{\frac{D}{\Pi \cdot t}}\right] \tag{26}$$

r – particle radius
D – diffusion coefficient for C, or Mn, or Ni.

Expression 1/r is a result of stationary diffusion field while as $t^{-0,5}$ is related to intermediate diffusion field with different concentration. After long dissolution time the intermediate part of equation may be omitted. Then we receive equation (27)

$$r^2 = r_o^2 - 2\,\alpha\, D \cdot t \tag{27}$$

r_o – initial particle radius,
α - non-dimensional parameter of over saturation given by (28)

$$\alpha = \frac{C_S - C_m}{C_P - C_S} \tag{28}$$

The above equations are valid if there is no interaction of diffusional fields from neighboring particles. For r = 0 time needed for dissolution of spherical particle $(FeMn)_3C$ at temperature higher than A_{C_1} is given from relation (29)

$$t_d = \frac{r_o^2}{2\,\alpha\, D} = \frac{r_o^2}{2\,D}\frac{C_P - C_S}{C_S - C_m} \tag{29}$$

Volumetric fraction of particles as function of time is given by (30).

$$f = f_o\left(\frac{r}{r_o}\right)^3 \equiv f_o\left(1 - \frac{2\,\alpha\, D \cdot t}{r_o^2}\right)^{3/2} \tag{30}$$

f_o – initial volume fraction of particles

For D i r_o = 1.5 μm at temperature 850^0C time for dissolution of cementite particle for analytical calculation is 0.36 s, and for numerical resolution equals 0.48 s.

For dissolution problems, kinetics of the reaction is ussually presented as relation (31)

$$f / f_o \cong 1 - c_2 \cdot \alpha \cdot (\tau)^{n_1} \tag{31}$$

where: c_2 – is material constant
n_1 – power exponent for most cases taken as n = 0,5.
τ - time of reaction

Because dissolved layer is assume to be the surrounding austenite the above equations are equated to Avrami relationship (32)

$$f / f_o = X = 1 - \exp(-k \cdot t_n) \tag{32}$$

X – volume fraction of austenite,
t – time of transformation at constant temperature.

For conditions n ≅ 1- nucleation of austenite at interphase surfaces and on the grain boundaries and early stages of nucleation at one dimensional growth the amount of austenite X which has formed in the place of former carbide particles is given by relationships (33) and (34).

$$X = 1 - \exp(-k \cdot t) = 1 - \exp\left(-\frac{k \cdot r_o^2}{2\,\alpha\, D}\right) \tag{33}$$

$$X = 1 - \exp\left(-\frac{k \cdot r_o^2}{2\ D} \cdot \frac{C_P - C_S}{C_S - C_m}\right) \tag{34}$$

5. Chemical analysis in micro-areas

The chemical composition of the microstructural constituents of the multiphase 6Mn16 steel was determined by analytical STEM point analysis with EDAX system attached to Philips CM20 transmission electron microscope.

Morphologies of bainite – martensite – retained austenite islands in ferrite matrix as observed in electron transmission microscope are presented in Figure 6 a, b, and c. In Fig. 6 a the overall distribution of BMA islands in ferrite matrix is shown. The BMA islands are usually smaller than 1 μm in diameter. They were formed after fast cooling from intercritical temperature 750°C. In some of them (Fig. 6 b and Fig. 6 c) micro-twins are visible. It means that higher carbon content than 0.3%C is present in islands because such amount of carbon causes formation of twins in martensitic areas [16].

Partitioning of C and subtitutional elements like Mn and Ni had taken place during 1800 s at temperature 750°C. The increased concentration of manganese, chromium and nickel in islands was confirmed by mapping analysis shown in Figure 7. Mainly Mn was partitioned between ferrite matrix and BMA islands. Detailed mass % concentrations of elements in BM and BMA islands are given in Table 3. Based on that analysis chromium is the only element which had not undergone partitioning at at 750°C/1800 s. The characteristic X –ray point analysis from ferrite and bainite –martensite islands are given in Table 3.

Table 3.
Point chemical analysis of ferrite matrix and BM and BMA islands in 6Mn16 steel after annealing at 750^{0}C/1800s

Element	Concentration of element in mass %			
	Ferrite matrix	BM island	BMA island	BM island
Fe	95.8	93.9	92.6	93.5
Mn	2.7	4.5	5.7	4.8
Ni	0.5	0.6	0.7	0.7
Cr	1.0	1.0	1.0	1.0

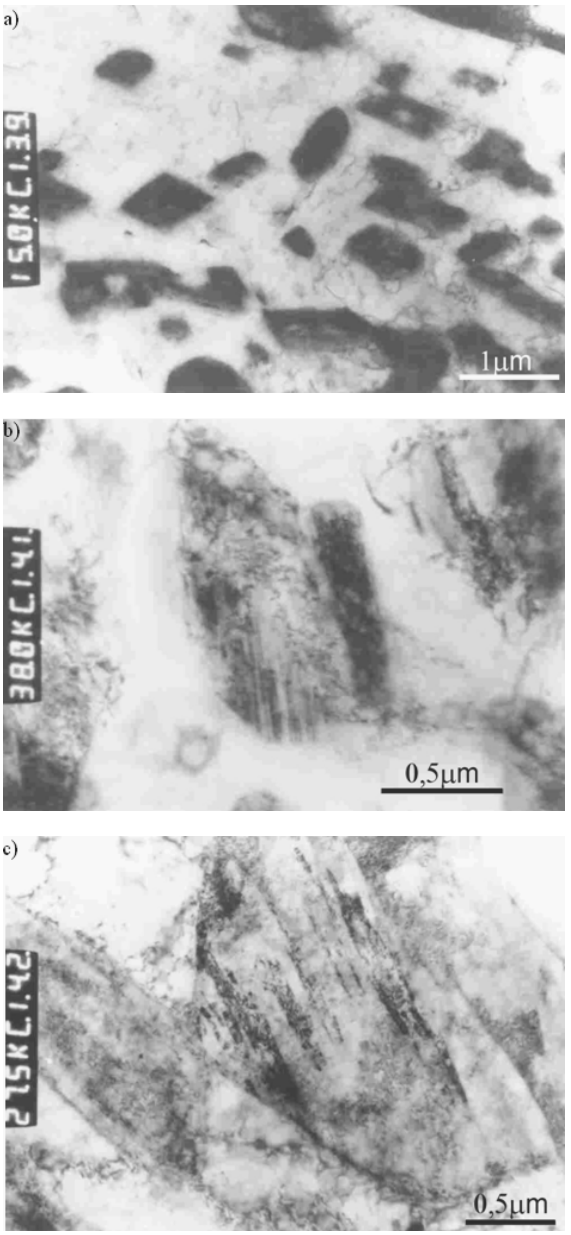

Fig. 6. a) morphology of bainite-martensite islands b) interior microstructure of bainite-martensite-austenite islands –BMA c) micro twins in BMA island

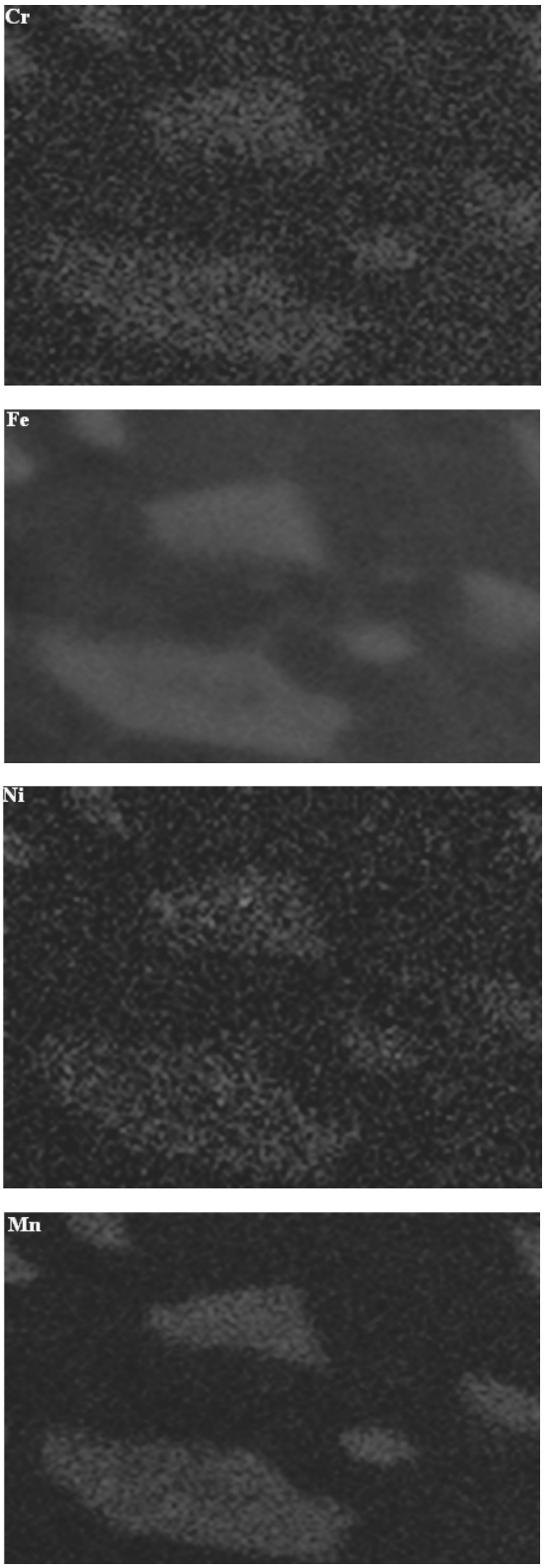

Fig. 7. Mapping analysis of substitional elements in BMA islands of 6Mn16 steel after annealing at 750°C/1800 s

6. Conclusions

Mn partitioning between ferrite and cementite during soft annealing at temperature 625°C before intercritical heat treatment had influence on the kinetic of austenite formation during the course of phase transformation $\alpha \rightarrow \gamma$.

It has been shown that soft annealing before intercritical heat treatment in the $(\alpha+\gamma)$ temperature range affected value of the parameter "k" which is responsible for advancement of the phase transformation.

At the first stage of diffusion controlled phase transformation, the growth of the isolated austenite islands was observed for those which met conditions for the nucleation at the beginning of transformation.

At further stage of transformation the continuous nucleation at the grain boundaries and interfaces of α/α and α/cementite takes place at the preferential sites for heterogeneous nucleation and growth of γ phase in α ferrite matrix. This situation corresponds to n=1 in J-M equation.

The increase in soft annealing time from 1-60 hours at 625°C increases Mn partitioning between ferrite and cementite and new formed austenite and decreases the rate of the austenite formation during next intercritical annealing in the $(\alpha+\gamma)$ temperature range at 700 and 750°C.

Saturation of carbides with Mn caused their slower dissolution and reduced the progress of $\alpha \rightarrow \gamma$ transformation as well as grain growth.

The general equations for carbide dissolution and austenite formation processes were given.

References

[1] A.K. Lis, J. Lis; Effect of hot deformation and cooling rate on phase transformations in low carbon HN5MVNb bainitic steel, Trans Tech Publications, Materials Science Forum 539-543 (2007) 4620-4625.

[2] J. Lis, A.K. Lis, C. Kolan, Processing and properties of C-Mn steel with dual-phase microstructure, Journal of Materials Processing Technology 162-163 (2005) 350-357.

[3] B. Gajda, A.K. Lis, Intercritical annealing with isothermal holding of TRIP CMnAlSi steel, Journal of Achievements in Materials and Manufacturing Engineering 20 (2007) 439-442.

[4] N. Wolańska, A.K. Lis, J. Lis, Investigation of C-Mn-B steel after hot deformation, Archives of Materials Science and Engineering 28/2 (2007) 119-125.

[5] A.K. Lis, B. Gajda, J. DeArdo, New steel chemistry design for TRIP and Dual Phase structures, Materials Science and Technology 2005, Pittsburgh, USA

[6] S.K. Chang, J.H. Kwak, Effect of Manganese on Aging in Low Carbon Sheet Steels, Iron And Steel Institute Of Japan International 37 (1997) 74-79.

[7] K. Eberle, P. Cantinieaux, P. Harlet, New thermomechanical strategies for the production of high strength low alloyed multiphase steel showing a TRIP effect, Steel Research 70/6 (1999) 233-238.

[8] G. Michta, J. Pietrzyk, W. Osuch, A. Kruk, Stability of retained austenite at low temperature in low carbon cooper bearing steels with TRIP assisted effect, Materials Engineering 25/3 (2003) 339-342 (in Polish).

[9] G. Michta, W.Osuch, A. Kruk, Testing of isothermal tranformation of undercooled austenite within 380-650°C temperature range in low carbon steels with containing manganese and silicon, Metallurgist – Information Metallurgical 4 (2003) 171-176 (in Polish).

[10] S. Sun, M. Pugh, Manganese partitioning in dual phase steel during annealing, Materials Science and Engineering A276 (2000) 187-174.

[11] J. Lis, J. Morgiel, A. Lis, The effect of Mn partitioning in Fe-Mn-Si alloy investigated with STEM-EDS techniques, Materials Chemistry and Physics 81 (2003) 466-468.

[12] J. Lis, Microsegregation of manganese in low carbon steels during intercritical heat treatments, Publisher WIPM and FS, Czestochowa University of Technology, Seria: Materials Engineering, No 7, Częstochowa, 2005 (in Polish).

[13] Z. Kędzierski, Phase transformations in condensed systems, Academia Publisher AGH, Krakow, 2003 (in Polish).

[14] G. Guy, Introduction to Materials Science, PWN, Warszawa, 1970 (in Polish).

[15] J. Pietrzyk, G. Michta, A. Kruk, Kinetics of bainite transformation of austenite formed after annealing in temperature range $A_1 - A_3$ in steel 0,2%C, 1,5%Mn, 1,5% Si, Metallurgist – Information Metallurgical 5 (1997) 218-222.

[16] R. Zenker, Martensitarten und Martensitmorphologie in Eisenlegierungen, Neue Hütte 18/4 (1973) 216-223.

[17] N. Pussegoda, W.R. Tyson, P. Wycliffe, G.R. Purdy, Metallurgical Transactions 15A (1984) 1499-1507.

[18] J. Agren, Kinetics of carbide dissolution, Scandinavian Journal of Metallurgy 19 (1990) 2-8.

[19] J. Lis, A. Lis, Kinetics of the austenite formation during intercritical annealing, Journal of Achievements in Materials and Manufacturing Engineering (2008) (in Print).